

ARCHIVES
of
FOUNDRY ENGINEERING

ISSN (2299-2944)
Volume 2020
Issue 2/2020

31 – 36

10.24425/afe.2020.131298

5/2



Published quarterly as the organ of the Foundry Commission of the Polish Academy of Sciences

The Effect of Metal Pouring Conditions on the Formation of Defects in the Casting

L. Sowa *, T. Skrzypczak, P. Kwiaton

Institute of Mechanics and Machine Design Fundamentals, Czestochowa University of Technology
Dabrowskiego 73, 42-200 Czestochowa, Poland

* Corresponding author. E-mail address: sowa@imipkm.pcz.pl

Received 27.06.2019; accepted in revised form 04.11.2019

Abstract

The mathematical model and numerical simulations of the solidification of a cylindrical casting, which take into account the process of the mould cavity filling by liquid metal and the feeding of the casting through the conical riser during its solidification, are proposed in the paper. The interdependence of thermal and flow phenomena were taken into account because they have an essential influence on solidification process. The effect of the pouring temperature and pouring velocity of the metal on the solidification kinetics of the casting was determined. In order to obtain the casting without shrinkage defects, an appropriate selection of these parameters was tried, which is important for foundry practice. The velocity fields have been obtained from the solution of Navier-Stokes equations and continuity equation, while temperature fields from solving the equation of heat conductivity containing the convection term. In the solidification modelling the changes in thermo-physical parameters as a function of temperature were considered. The finite element method (FEM) was used to solve the problem.

Keywords: Castings defects, Solidification process, Numerical modelling, Molten metal flow

1. Introduction

The growing requirements regarding the quality of castings require intensive technological development of foundry methods. The creation of the casting by the gravitational pouring of liquid metal into a metal mould was analyzed in this paper. Nowadays, much attention has recently been devoted also to other casting methods, mainly lost wax casting technology [1] or the continuous casting method [2, 3]. All activities improving casting methods are primarily aimed at obtaining high strength castings without casting defects or at least limiting them to sizes acceptable by customers. Conducting research on real objects is significantly difficult due to the lack of visibility and high temperatures taking place there, therefore computer simulations are becoming an increasingly common tool used to improve the casting methods [4-11]. However, they should be seen in synergy

with other methods to improve the quality and control of the castings, e.g. NDT methods. In this article, the process of casting solidification is analyzed, considering the phenomena of heat exchange and fluid flow, starting from the moment of filling the metal mould by molten metal and ending with the complete solidification of the casting. The shape of the solidus line is observed, assessing whether it has been closed in the casting area. Such a situation would mean the lack of supply of this area by the liquid metal from the riser and the formation of defects at this place of the casting. We try to avoid this situation by choosing the right velocity and temperature of pouring the molten metal into the mould. Therefore, the aim of the work was to evaluate the impact of metal pouring conditions into the cavity of metal mould on the solidification process of the casting, so that it arises without defects.

2. The mathematical description

In the mathematical model, it was adopted that molten metal has the properties of an incompressible viscous fluid and a heat-conducting, and its flow is globally laminar. It was also assumed that the solidification front is mushy, i.e. liquid metal solidifies in the liquidus/solidus temperature range. This model of solid phase growing is most commonly used when solidification of metal alloys is considered. The mathematical description of the casting solidification process considering the liquid metal movements is based on the solution of the following equations system in a cylindrical axial-symmetric coordinate system [4-9]

– the Navier-Stokes equations

$$\mu \left(\frac{\partial^2 v_r}{\partial r^2} + \frac{1}{r} \frac{\partial v_r}{\partial r} + \frac{\partial^2 v_r}{\partial z^2} - \frac{v_r}{r^2} \right) - \frac{\partial p}{\partial r} + \rho g_r + \rho g_r \beta (T - T_\infty)_r = \rho \frac{dv_r}{dt}, \quad (1)$$

$$\mu \left(\frac{\partial^2 v_z}{\partial r^2} + \frac{1}{r} \frac{\partial v_z}{\partial r} + \frac{\partial^2 v_z}{\partial z^2} \right) - \frac{\partial p}{\partial z} + \rho g_z + \rho g_z \beta (T - T_\infty)_z = \rho \frac{dv_z}{dt},$$

– the continuity equation

$$\frac{\partial v_r}{\partial r} + \frac{v_r}{r} + \frac{\partial v_z}{\partial z} = 0, \quad (2)$$

– the equation of heat conductivity with the convection term

$$\frac{\lambda}{r} \frac{\partial T}{\partial r} + \frac{\partial}{\partial r} \left(\lambda \frac{\partial T}{\partial r} \right) + \frac{\partial}{\partial z} \left(\lambda \frac{\partial T}{\partial z} \right) = \rho C_{ef} \frac{\partial T}{\partial t} + \rho C_{ef} \left(v_r \frac{\partial T}{\partial r} + v_z \frac{\partial T}{\partial z} \right), \quad (3)$$

– the volume fraction equation

$$\frac{\partial F}{\partial t} + v_r \frac{\partial F}{\partial r} + v_z \frac{\partial F}{\partial z} = 0, \quad (4)$$

where: λ - the thermal conductivity coefficient [W/(mK)], T - the temperature [K], $\rho = \rho(T)$ - the density [kg/m³], $\mu(T)$ - the dynamical viscosity coefficient [kg/(ms)], v_r, v_z - the r -component and z -component of velocity, respectively [m/s], $C_{ef} = c + L/(T_L - T_S)$ - the effective specific heat of a mushy zone [J/(kgK)], t - the time [s], L - the latent heat of solidification [J/kg], g_r, g_z - the r - and z -component of gravitational acceleration, respectively [m/s²], p - the pressure [N/m²], β - the volume coefficient of thermal expansion [1/K], c - the specific heat [J/(kgK)], r, z - the coordinates of the vector of the considered node's position [m], r - the radius [m], T_∞ - the reference temperature ($T_\infty = T_{in}$) [K], F - the pseudo-concentration function across the elements lying on the free surface.

The equations (1-4) are completed by appropriate boundary conditions and initial conditions.

The initial conditions for temperature and velocity fields are given as [6-9]

$$\begin{aligned} \mathbf{v}(r, z, t_0) = \mathbf{v}_0(r, z) &= v_{in} \Big|_{\Gamma_{1-1}}, \\ T(r, z, t_0) = T_0(r, z) &= \begin{cases} T_{in} & \text{on } \Gamma_{1-1} \\ T_A & \text{in } \Omega_A \\ T_M & \text{in } \Omega_M \end{cases} \end{aligned} \quad (5)$$

The boundary conditions, specified in the considered problem, on the indicated surfaces (Fig. 1), were as follows

- for velocity [6, 7, 9]

$$v_n \Big|_{\Gamma_{1-1}} = v_{in}, \quad v_t \Big|_{\Gamma_{1-1}} = v_t \Big|_{\Gamma_{2-2}} = v_n \Big|_{\Gamma_{2-2}} = 0, \quad v_n \Big|_{r=0} = 0, \quad (6)$$

$$\frac{\partial v_t}{\partial n} \Big|_{r=0} = 0, \quad v_n \Big|_{\Gamma_G} = 0, \quad v_t \Big|_{\Gamma_G} = 0,$$

- for temperature [6-11]

$$T \Big|_{\Gamma_{1-1}} = T_{in}, \quad \frac{\partial T}{\partial n} \Big|_{r=0} = 0, \quad \frac{\partial T}{\partial n} \Big|_{\Gamma_{2-2}} = 0,$$

$$\lambda_S \frac{\partial T_S}{\partial n} \Big|_{\Gamma_{G-}} = \lambda_G \frac{\partial T_G}{\partial n} \Big|_{\Gamma_{G-}}, \quad (7)$$

$$\lambda_G \frac{\partial T_G}{\partial n} \Big|_{\Gamma_{G+}} = \lambda_M \frac{\partial T_M}{\partial n} \Big|_{\Gamma_{G+}},$$

$$\lambda_M \frac{\partial T_M}{\partial n} \Big|_{\Gamma_M} = -\alpha_M (T_M \Big|_{\Gamma_M} - T_a),$$

where: T_a - the ambient temperature [K], α_M - the heat transfer coefficient between the ambient and the mould [W/(m²K)], T_A - the temperature of air inside mould cavity in initial state [K], T_{in} - the initial temperature [K], T_M, T_G, T_S - the temperature of mould, gap (protective coating) and solid phase, respectively [K], v_{in} - the initial velocity [m/s], $\lambda_M, \lambda_S, \lambda_G$ - the thermal conductivity coefficient of mould, solid phase and gap, respectively [W/(mK)], n - the outward unit normal surface vector, v_t, v_n - the tangential and normal component of velocity vector, respectively [m/s].

In the applied of solid phase growth model, the internal heat source is not visible in the heat conduction equation (3) because it is in the effective specific heat of two-phase area [6-9]. The above equations have been solved with the FEM in the weighted residuals formulation [6-9].

3. Numerical calculations

To analyse the impact of the movements of the liquid metal alloy and pouring conditions on solidification of the casting, the following casting-mould system was considered (Fig. 1). The

outside mould dimensions are equal to: $d=0.320\text{m}$, $h=0.280\text{m}$ [m], whereas the mould cavity dimensions are equal to: $d_o=0.200\text{m}$, $h_o=0.070\text{m}$, $h_n=0.150\text{m}$, $d_{ni}=0.080\text{m}$, $d_{ns}=0.100\text{m}$, $d_{in}=0.020\text{m}$. The internal surface of the steel mould is covered with a protective coating with 2mm thickness. This layer was modelled using an additional area with protective coating properties.

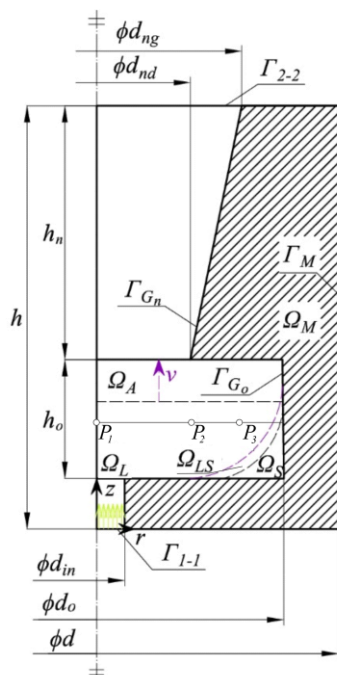


Fig.1. Considered system and identification of regions

The numerical calculations were carried out for the casting made of low-carbon cast steel and the steel mould. The thermo-physical properties were taken from work [3, 7-9] and are summarised in Table 1 for casting and Table 2 for other regions under consideration.

Table 1.

Material properties of the casting - cast steel

Material property	Liquid phase	Solid phase
ρ [kg/m ³]	7300	7800
c [J/(kgK)]	830	644
λ [W/(mK)]	23	45
μ [kg/(ms)]	0.006	10000
β [1/K]	0,00014	
Additional parameters		
T_L [K]		1810
T_S [K]		1760
L [J/kg]		270000

The overheated metal with temperature $T_{in}=1820$ or 1835K has been poured from the bottom with the velocity $v_{in}=0.1$ or 0.2 m/s, depending on the variant, into the steel mould with initial temperature $T_M=350\text{K}$. Other important temperatures were equal to: $T_A=350\text{K}$, $T_a=300\text{K}$. The heat transfer coefficient (α) between ambient and the mould was equal to $\alpha_M=200\text{W}/(\text{m}^2\text{K})$.

Table 2.

Material properties used in the calculations for other regions

Material property	Mould	Protective coating	Air
ρ [kg/m ³]	7200	1600	1.23
c [J/(kgK)]	600	1670	1006
λ [W/(mK)]	42	0.3	0.024
μ [kg/(ms)]	-	-	0.000018

The analysis of the solidification process was carried out using a professional Fidap program. This software ensures fast convergence of numerical calculations during the simulation of filling the mould by molten metal. The geometry of considered system was divided into 4979 quadrilateral elements.

4. Discussion of the numerical simulations results

A lot of numerical simulations were done to determine the influence of liquid metal movements and parameters of its pouring into a metal mold on the obtaining process of a casting without shrinkage defects. Assuming intensive cooling of the casting-mould system, efforts were made to ensure directional solidification of the casting. The analysis of heat exchange phenomena and fluid flow was made starting from the moment of filling the metal mould by molten metal (Figs 2 and 3), through the convective movements of liquid metal (Fig. 4) and ending with the complete solidification of the casting (Figs 5-7).

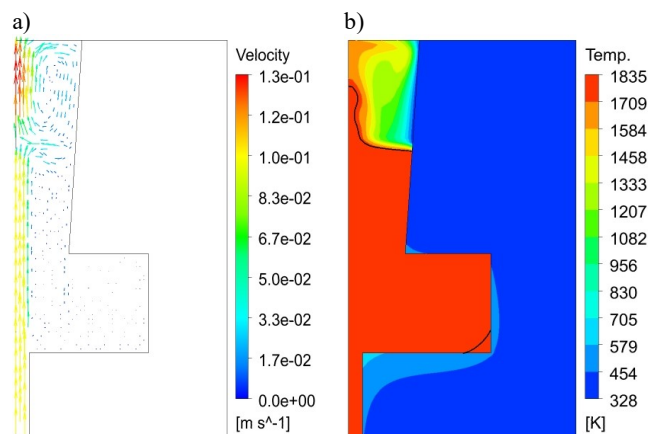


Fig.2. The velocity vectors (a) and temperature distribution (b) at $t=86\text{s}$, I variant

Numerical calculations of the solidification process of the casting-riser system were carried out at different combinations of pouring parameters from which the system of three pairs of velocity and pouring temperature was selected, creating the following variants. In I variant they were: $v_{in}=0.1\text{m/s}$, $T_{in}=1835\text{K}$. In II variant they were equal to: $v_{in}=0.1\text{m/s}$, $T_{in}=1820\text{K}$ and in III variant they equivalent to: $v_{in}=0.2\text{m/s}$, $T_{in}=1835\text{K}$. Filling the mould with liquid metal is shown in the form of velocity vectors distributions for selected moments of time. Figure 2a shows the velocity field when the free surface of the poured metal from below is in the half of the riser height (after $t=86\text{s}$). The temperature field corresponding to this time step is shown in Figure 2b. We see here significant metal movement only along the symmetry axis of the casting and its small movements in the rest of the casting (Fig. 2a). This way of metal flow filling the mould cavity is confirmed by velocity distributions made along the radius in the half of the casting height for selected moments of time: $t=71\text{s}$, $t=86\text{s}$ and $t=107\text{s}$ (Fig. 3b). These time steps correspond respectively to the moments when the liquid metal completely fills the casting area, when the conical riser is filled to half and when the system is completely full. At the same time steps, the temperature distributions along the casting radius in half of its height are shown in Figure 3a. We can see that the pouring temperature is maintained only in the main stream of the flowing metal and in the rest of the casting there is a systematic decrease with the time of filling the mould cavity. The temperature on the wall of the casting, in the half of its height, is higher than the solidus temperature. This means that the solid phase of the casting has not yet been formed at this place during the mould cavity filling process. In turn, observing the solidus line on the temperature distribution (Fig. 2b), you can see solidification of the casting only in its lower corner, during this period of casting formation.

After filling the mould cavity with liquid metal, the forced metal flow disappears and only natural convection movements can be observed, which are shown in Figure 4a at a selected moment of simulation time ($t=400\text{s}$). This velocity field corresponds to the temperature field shown in Figure 4b on which a solidus line was drawn separating the solid-liquid area of the casting from its solidified area.

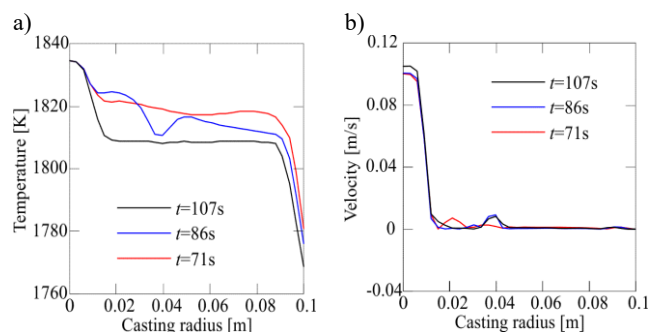


Fig.3. Distributions of temperature (a) and velocity (b) along the radius of the casting in half of its height in selected time steps: $t=71\text{s}$, $t=86\text{s}$, $t=107\text{s}$, I variant

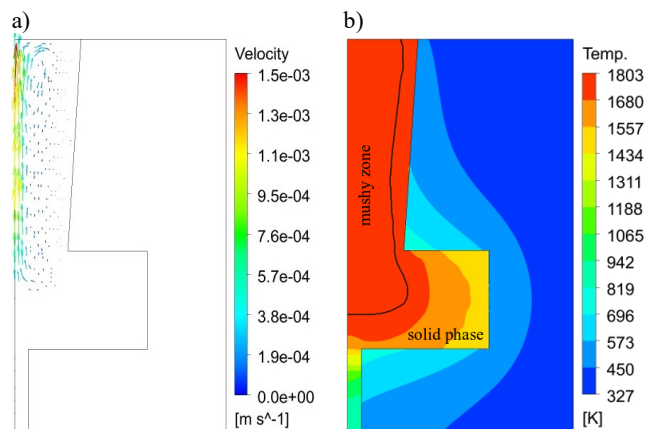


Fig.4. The velocity vectors (a) and temperature distribution (b) at $t=400\text{s}$, I variant

Then, the temperature fields after casting solidification were compared for three variants of pouring parameters, observing the shape of the solidus line in the final solidification steps of the casting-riser system (Figs 5-7). When the solidus line is closed in the casting, the area limited by it will not be fed with liquid metal from the riser and in this place, as a result of metal shrinkage, a shrinkage defect will occur. It can therefore be concluded that the casting has been damaged in this place, which is the case of variants II and III (Figs 6 and 7). This means that the pouring temperature was too low in II variant and the pouring velocity was too large in III variant. However, we try to avoid such a situation and move such a defect to the riser choosing the right pouring parameters, which was successful in variant I (Fig. 5).

Sample cooling curves of the considered alloy at points 1, 2 and 3 of the casting for I variant of pouring conditions were made (Fig. 8). The location of the points is shown in Figure 1, and their coordinates in the considered coordinate system (r, z) were respectively: $P_1(0.0, 0.095)$, $P_2(0.040, 0.095)$, $P_3(0.070, 0.095)$.

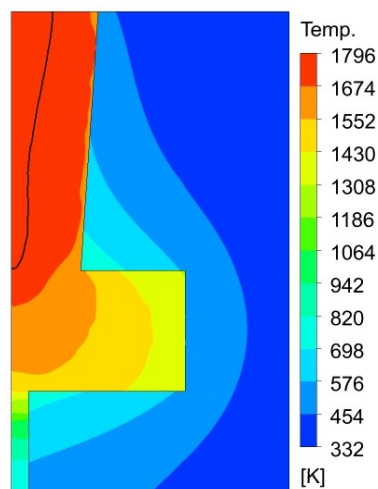


Fig.5. Temperature field after solidification of the casting: $t=537\text{s}$, I variant

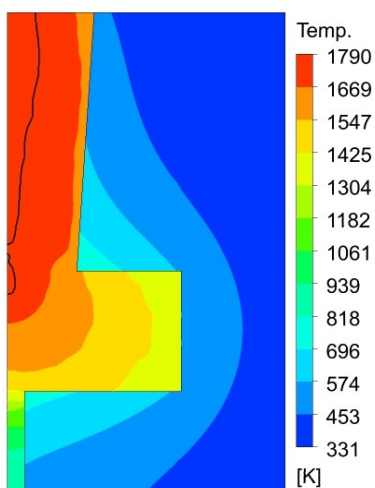


Fig.6. Temperature field after solidification of the casting: $t=527s$, II variant

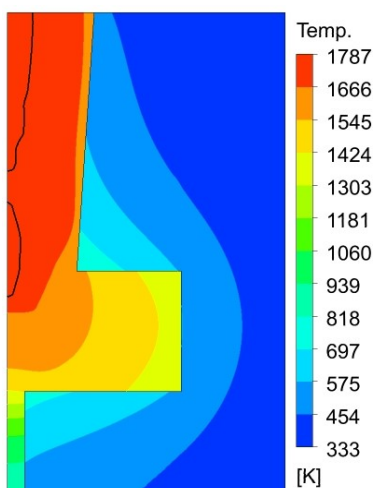


Fig.7. Temperature field after solidification of the casting: $t=507s$, III variant

The course of temperature change as a function of time confirms the logic of the obtained numerical simulation results. After a period of temperature increase caused by filling the cavity of the mould, it slowly decreases, then the metal solidifies and the temperature rapid decrease due to the outflow of heat to the mould. It can also be seen that the temperature decreases faster below the solidus temperature at points closer to the wall of the casting. In point 1 a constant temperature maintains throughout the period of filling the mould cavity, while at the other points it decreases during this time due to the slight movements of the molten metal at their place of location.

In turn, analysing the course of the temperature change curve at point 1, for three variants of pouring conditions, you can see a shorter time of filling the mould cavity in the variant 3 due to a greater velocity of metal pouring (Fig. 9).

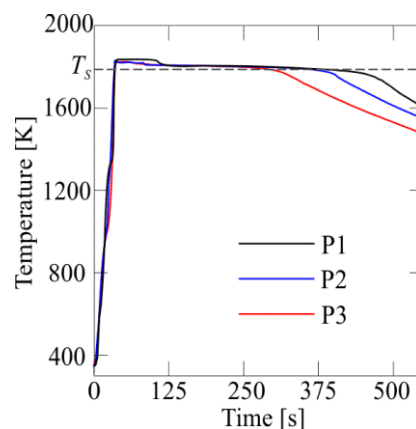


Fig.8. Examples of the cooling curves of the considered alloy at point 1, 2 and 3 of the casting for I variant of pouring conditions

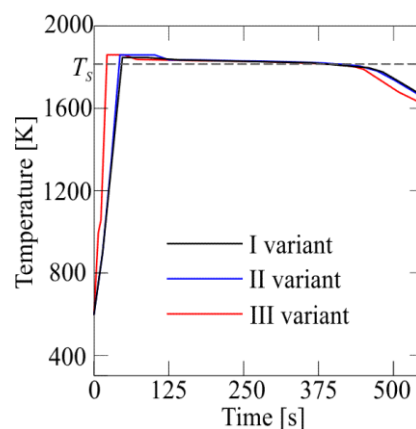


Fig.9. Examples of the cooling curves of the considered alloy at point 1 of the casting for three variants of pouring conditions

5. Conclusions

The mathematical model and numerical simulation results of the casting solidification which consider filling process of the mould cavity by molten metal were presented in this paper. The influence of molten metal motions on the solidification kinetics and the location of the end of casting solidification were evaluated. The numerical calculations were made for three variants of metal pouring parameters. It has been observed that the solidification process begins effectively for this shape of the casting when the mold cavity is completely filled with liquid metal. However, at the final solidification time of the casting-riser system, the solidus line closed at the upper part of the casting is visible. This suggests the formation of shrinkage defects at this place if the casting process was performed at a reduced pouring temperature or with an increased pouring velocity of molten metal (Figs 6 and 7). This situation was not observed if casting process was made at standard pouring parameters of the mould cavity (Fig. 5). In this case, the solidification end took place in the riser, which is desired, because the riser is cut off and re-processed. It

also proves that the conical-shaped riser executed its task and the casting was made without casting defects.

References

- [1] Grzeškowiak, K., Wojciechowski, M. & Sytek K. (2013). The effect of the method of pouring liquid metal into mould on misrun formation in the castings made with lost-wax casting technology. *Archives of Mechanical Technology and Automation*. 33(4), 15-19.
- [2] Szajnar, J., Stawarz, M., Wróbel, T., Sebzda, W., Grzesik, B. & Stępień M. (2010). Influence of continuous casting conditions on grey cast iron structure. *Archives of Materials Science and Engineering*. 42(1), 45-52.
- [3] Miłkowska-Piszczek, K. & Korolczuk-Hejnak M. (2013). An analysis of the influence of viscosity on the numerical simulation of temperature distribution as demonstrated by the CC process. *Archives of Metallurgy and Materials*. 58 (4), 1263-1274. DOI: 10.2478/amm-2013-0146.
- [4] Eriksson, R., Jonsson, L. & Jönsson P.G. (2004). Effect of entrance nozzle design on the fluid flow in an ingot mold during filling. *ISIJ International*. 44(8), 1358-1365.
- [5] Huang, P-H. & Lin C-J. (2015). Computer-aided modeling and experimental verification of optimal gating system design for investment casting of precision rotor. *International Journal of Advanced Manufacturing Technology*. 79(7-8), 997-1006. DOI: 10.1007/s00170-015-6897-5.
- [6] Lewis, R.W., Postek, E.W., Han, Z. & Gethin D.T. (2006). A finite element model of the squeeze casting process. *International Journal of Numerical Methods for Heat & Fluid Flow*. 16(5), 539-572. DOI: 10.1108/09615530610669102.
- [7] Dyja, R., Gawrońska, E. & Grosser A. (2018). A computer simulation of solidification taking into account the movement of the liquid phase. *MATEC Web of Conferences*. 157, 1-9. DOI: 10.1051/mateconf/201815702008.
- [8] Skrzypczak, T., Węgrzyn-Skrzypczak, E. & Sowa L. (2018). Numerical modeling of solidification process taking into account the effect of air gap. *Applied Mathematics and Computation*. 321, 768-779. DOI: 10.1016/j.amc.2017.11.023.
- [9] Sowa, L., Skrzypczak, T. & Kwiaton P. (2019). Computer evaluation of the influence of liquid metal movements on defects formation in the casting. *MATEC Web of Conferences*. 254, 1-9. 02017. DOI: 10.1051/mateconf/201925402017.
- [10] Nadolski, M., Zyska, A., Konopka, Z., Łągiewka, M. & Karolczyk J. (2011). The assessment of bell casting producibility based on computer simulation of pouring and solidification. *Archives of Foundry Engineering*. 11(3), 141-144.
- [11] Perzyk, M., Kochański, A., Mazurek, P. & Karczewski K. (2014). Selected principles of feeding systems design: simulation vs industrial experience. *Archives of Foundry Engineering*. 14(4), 77-82.